Heriot-Watt University

Heriot-Watt University
Research Gateway

Aberration corrections for free-space optical communications in atmosphere turbulence using orbital angular momentum states

Zhao, S. M.; Leach, Jonathan; Gong, L. Y.; Ding, J.; Zheng, B. Y.

Link to publication in Heriot-Watt Research Gateway

Aberration corrections for free-space optical communications in atmosphere turbulence using orbital angular momentum states

S. M. Zhao,[1,2,*] **J. Leach,**[3] **L. Y. Gong,**[1] **J. Ding,**[1] **and B. Y. Zheng**[1]

[1]*Institute of Signal Processing and Transmission, Nanjing University of Posts and Telecommunications, Nanjing, China*
[2]*Key Lab of Broadband Wireless Communication and Sensor Network Technology (Nanjing University of Posts and Telecommunications), Ministry of Education, China*
[3]*Department of Physics and Astronomy, SUPA, University of Glasgow, Glasgow, UK*
*zhaosm@njupt.edu.cn

Abstract: The effect of atmosphere turbulence on light's spatial structure compromises the information capacity of photons carrying the Orbital Angular Momentum (OAM) in free-space optical (FSO) communications. In this paper, we study two aberration correction methods to mitigate this effect. The first one is the Shack-Hartmann wavefront correction method, which is based on the Zernike polynomials, and the second is a phase correction method specific to OAM states. Our numerical results show that the phase correction method for OAM states outperforms the Shark-Hartmann wavefront correction method, although both methods improve significantly purity of a single OAM state and the channel capacities of FSO communication link. At the same time, our experimental results show that the values of participation functions go down at the phase correction method for OAM states, i.e., the correction method ameliorates effectively the bad effect of atmosphere turbulence.

OCIS codes: (010.1285) Atmospheric correction; (060.2605) Free-space optical communication; (070.6120) Spatial light modulators.

References and links

1. L. Allen, M. Beijersbergen, R. Spreeuw, and J. Woerdman, "Orbital angular momentum of light and the transformation of Laguerre-Gaussian laser modes," Phys. Rev. A **45**, 8185–8189 (1992).
2. J. Wang, J. Yang, I. Fazal, N. Ahmed, Y. Yan, B. Shamee, A. Willner, K. Birnbaum, J. Choi, B. Erkmen, S. Dolinar, and M. Tur, "Demonstration of 12.8-bit/s/Hz spectral efficiency using 16-QAM signals over multiple orbital-angular-momentum modes," in 37th European Conference and Exhibition on Optical Communication, paper We.10.P1.76 (2011).
3. I. Djordjevic, "Deep-space and near-Earth optical communications by coded orbital angular momentum (OAM) modulation," Opt. Express **19**, 14277–14289 (2011).
4. I. Djordjevic and M. Arabaci, "LDPC-coded orbital angular momentum (OAM) modulation for free-space optical communication," Opt. Express **18**, 24722–24728 (2010).
5. M. Gruneisen, W. Miller, R. Dymale, and A. Sweiti, "Holographic generation of complex fields with spatial light modulators: application to quantum key distribution," Appl. Opt. **47**, A32–A42 (2008).
6. J. Garcia-Escartin and P. Chamorro-Posada, "Quantum multiplexing with the orbital angular momentum of light," Phys. Rev. A **78**, 062320 (2008).
7. G. Gibson, J. Courtial, M. Padgett, M. Vasnetsov, V. Pas'ko, S. Barnett, and S. Franke-Arnold, "Free-space information transfer using light beams carrying orbital angular momentum," Opt. Express **12**, 5448–5456 (2004).

8. C. Paterson, "Atmospheric turbulence and orbital angular momentum of single photons for optical communication," Phys. Rev. Lett **94**, 153901 (2005).
9. J. Anguita, M. Neifeld, and B. Vasic, "Turbulence-induced channel crosstalk in an orbital angular momentum-multiplexed free-space optical link," Appl. Opt. **47**, 2414–2429 (2008).
10. G. Tyler and R. Boyd, "Influence of atmospheric turbulence on the propagation of quantum states of light carrying orbital angular momentum," Opt. Lett. **34**, 142–144 (2009).
11. Y. X. Zhang and J. Chang, "Effects of turbulent aberrations on probability distribution of orbital angular momentum for optical communication," Chin. Phys. Lett. **26**, 074220 (2009).
12. C. Gopaul and R. Andrews, "The effect of atmospheric turbulence on entangled orbital angular momentum states," New J. Phys. **9**, 94 (2007).
13. S. Zhao, J. Leach, and B. Zheng, "Correction Effect of Shark-Hartmann Algorithm on Turbulence Aberrations for free space Optical Communications Using Orbital Angular Momentum," in 12th IEEE International Conference on Communication Technology (ICCT), pp. 580–583 (2010).
14. L. Andrews and R. Phillips, *Laser Beam Propagation through Random Media* (SPIE Press, 2005).
15. R. Hill, "Models of the scalar spectrum for turbulent advection," J. Fluid Mech. **88**, 541–562 (1978).
16. J. Strasburg and W. Harper, "Impact of atmospheric turbulence on beam propagation," Proc. SPIE **5413**, 93 (2004).
17. R. Frehlich, "Simulation of laser propagation in a turbulent atmosphere," Appl. Opt. **39**, 393–397 (2000).
18. M. Mahdieh, "Numerical approach to laser beam propagation through turbulent atmosphere and evaluation of beam quality factor," Opt. Commun. **281**, 3395–3402 (2008).
19. B. Platt, "History and principles of Shack-Hartmann wavefront sensing," J. Refract. Surg. **17**, 573–577 (2001).
20. V. Voitsekhovich, "Hartmann test in atmospheric research," J. Opt. Soc. Am. A **13**, 1749–1757 (1996).
21. A. Jesacher, A. Schwaighofer, S. Frhapter, C. Maurer, S. Bernet, and M. Ritsch-Marte, "Wavefront correction of spatial light modulators using an optical vortex image," Opt. Express **15**, 5801–5808 (2007).
22. R. Bowman, "Aberration correction for spatial light modulators," Master's thesis (Churchill College, 2007).
23. P. Vontobel, A. Kavcic, D. Arnold, and H. Loeliger, "A generalization of the Blahut–Arimoto algorithm to finite-state channels," IEEE Trans. Inf. Theory **54**, 1887–1918 (2008).
24. J. R. Fienup and J. J. Miller, "Aberration correction by maximizing generalized sharpness metrics," J. Opt. Soc. Am. A **20,** 609–620 (2003).

1. Introduction

In 1992, Allen *et. al.* showed that light can carry orbital angular momentum (OAM), and that an azimuthal phase dependence $exp(il\theta)$ of a light beam corresponds to ℓ units of OAM [1]. In principle, there is an infinite number of OAM eigenstates by a single-photon, which offer the possibilities of realizing arbitrary base-N quantum digits per single photon for free space optical communications (FSO) and quantum communications [2–5]. In contrast to the polarization degree of freedom, which provides only a two dimensional Hilbert space, OAM states of one photon may carry more information. Furthermore, the orthogonality among beams with different OAM states allows a simultaneous information transmission by different users with their own separate states [6]. At the same time, experiments demonstrated the possibility of information transmission using OAM states [7], and the information encoded in OAM states was resistant to any eavesdropping. Therefore, OAM states provide a promising method to increase the transmission rates and the security of FSO and quantum communications.

On the other hand, the purity of the modes is susceptible to spatial aberrations in free space, because an OAM state is associated with the spatial distribution of the wave-functions. Recently, the effect of an atmosphere turbulence on a free-space OAM communication channel has attracted a lot of attentions [8–12]. For example, the channel capacity for a communication link employing OAM states of a single photon under turbulent aberration was addressed in [8]. The channel crosstalk induced by turbulence was discussed in [9]. The effect of atmosphere turbulence on the propagation of quantum OAM states was presented in [10]. Turbulent tilt aberration being the maximum OAM measurement probabilities of photons among those turbulent effects was analyzed in details in [11]. Moreover, the effect of atmosphere turbulence on entangled OAM states was addressed in [12]. All these papers have discussed the decoherence effect of turbulent aberration on OAM states. We have used the Shark-Hartmann algorithm to

correct an OAM state damaged by turbulence aberration in [13]. However, an important question, namely how to more effectively mitigate such effects, has been so far much less analyzed and reported.

In this paper, we first shortly review turbulent aberrations and the two phase correction methods. Then, we study an atmospheric turbulence model [14, 15] and discuss the two methods to mitigate the decoherence effect of turbulent aberrations by numerical simulations. One is the Shack-Hartmann wavefront correction method, and the other is a phase correction method for OAM states. Finally, we testify the phase correction method for OAM states by experiments.

2. Turbulent aberrations and phase correction methods

The spatial variation in atmospheric aberration can be approximated using several thin sheets that modify the phase profile of the propagating beam. Usually, phase fluctuations result in amplitude fluctuations as the beam propagates. In simulations, the plane of the aberration can be modeled by an $N \times N$ array of random complex numbers with statistics that matches the fluctuations of the index of refraction. Many numerical methods have been proposed to simulate atmosphere turbulence [14–18]. Here, we use the model developed by Hill [15] and defined analytically by Andrews [14]. The spectrum of fluctuations in index of refraction $\Phi_n(k_x,k_y)$ is then given as

$$
\begin{aligned}
\Phi_n(k_x,k_y) \quad = \quad & 0.033C_n^2[1+1.802\sqrt{\frac{k_x^2+k_y^2}{k_l^2}} \\
& -0.254[\frac{k_x^2+k_y^2}{k_l^2}]^{-7/12}] \\
& \times \exp[\frac{k_x^2+k_y^2}{k_l^2}][k_x^2+k_y^2+\frac{1}{L_0^2}]^{-11/6},
\end{aligned}
\tag{1}
$$

where C_n^2 is the structure constant of the index of refraction, which represents the strength of turbulence, L_o^2 is the outer scale of turbulence that is the largest eddy size formed by injection of turbulent energy, $k_l = \frac{3.3}{l_0}$, l_0 is equals to the inner scale of turbulence, and k_i ($i=x,y$) is the wavenumber in i direction. Then, the phase spectrum $\Phi(k_x,k_y)$ is

$$
\Phi(k_x,k_y) = 2\pi k_0^2 \Delta Z \Phi_n(k_x,k_y),
\tag{2}
$$

where ΔZ is the spacing between the subsequent phase screens, and k_0 is the wavenumber of the light. The phase screen $\varphi(x,y)$ can be evaluated as the Fourier transform of a complex random distribution with the variance σ^2 as follows:

$$
\varphi(x,y) = FFT(C\sigma(k_x,k_y)),
\tag{3}
$$

and

$$
\sigma^2(k_x,k_y) = \left(\frac{2\pi}{N\Delta x}\right)^2 \Phi(k_x,k_y),
\tag{4}
$$

where C is an $N \times N$ array of complex random numbers with zero mean and variance one, and Δx is the grid spacing. Here, the grid spacing in x direction is assumed to be equal to that in y direction.

As we discuss later, phase distortion will be produced by atmosphere turbulence for a propagating beam. We use a retrieval algorithm to obtain the distortion phase, and consequently include the information about imperfections into the beam by some device, such as Spatial Light Modulation (SLM). This way we can obtain the 'perfect' image at the receiver.

In the following there are two retrieval algorithms. The first one is the Shack-Hartmann wavefront correction method (SH-algorithm), which is commonly used to reconstruct random phase distortions caused by the aberrations [19,20]. Its principle is based on the measurement of local slops incoming to the Hartmann mask wavefront. The mask wavefronts are mathematical functions called Zernike polynomials. Any wavefront $\varphi(x,y)$ can completely be described by a linear combination of Zernike polynomials $Z_0, Z_1, ..., Z_N$ [19]

$$\varphi(x,y) = \sum_{k=0}^{N} a_k Z_k(x,y). \tag{5}$$

Now, assuming that $\varphi(x,y)$ is the deformation wavefront caused by turbulent aberrations. By model estimation and using the least-squares method, the coefficients a_i can be obtained by solving the equantion

$$\varphi_x'(x,y) = \sum_{k=1}^{N} a_k Z_{kx}(x,y), \tag{6}$$

and

$$\varphi_y'(x,y) = \sum_{k=0}^{N} a_k Z_{ky}(x,y). \tag{7}$$

that is

$$\begin{pmatrix} G_x(1) \\ G_y(1) \\ \vdots \\ G_x(m) \\ G_y(m) \end{pmatrix} = \begin{pmatrix} D_{1x}(1) & \cdots & D_{nx}(1) \\ D_{1y}(1) & \cdots & D_{ny}(1) \\ \vdots & \cdots & \vdots \\ D_{1x}(m) & \cdots & D_{nx}(m) \\ D_{1y}(m) & \cdots & D_{ny}(m) \end{pmatrix} \begin{pmatrix} a_1 \\ \vdots \\ a_n \end{pmatrix}.$$

where, $G_x(m) = \varphi_x'(m)$, $G_y(m) = \varphi_y'(m)$, $D_{kx}(m) = Z_{kx}(m)$, and $D_{ky}(m) = Z_{ky}(m)$. This equation can be expressed in a simplified form

$$G = DA, \tag{8}$$

and the coefficients of Zernike polynomial A is can then be calculated by

$$A = D^{-1}G. \tag{9}$$

This way, we could get the phase of deformation wavefront caused by atmosphere turbulence using above coefficients and Eq. (5).

   The second retrieval algorithm is a phase correction method for OAM states, which is proposed to measure and correct the surface defects of beam by using Gerchberg-Saxton phase retrieval algorithm (GS-algorithm) [21]. GS-algorithm will deal there with the problem of finding the phase $\varphi(x,y)$ of a light field by just determining the modulus $A(k_x, k_y)$ of its Fourier transform as

$$A(k_x, k_y)exp[i\Phi(k_x, k_y)] = F\{exp[i\varphi(x,y)]\}. \tag{10}$$

In [21], $\varphi(x,y)$ corresponds to the hologram function, and $A(k_x, k_y)$ to the amplitude of the observed doughnut mode. GS-algorithm is iterative, and its procedure is as follows. A perfect phase spiral is used as a starting point, and the illumination beam profile is selected as the magnitude in the Spatial Light Modulation plane. A complex Fast Fourier Transform (FFT) is used to generate the phase in the diffraction plane. The magnitude part of a perfect ring is discarded and replaced with the distorted image generated by the SLM , and then transformed back to the SLM plane, where the magnitude is replaced with the illumination beam profile. After a few iterations of the loop, the phase will generally converge to a value, and the phase of the aberration can be retrieved. Moreover, it is shown that this retrieval algorithm can be implemented by experiment [22].

(a) Propagation through turbulent atmosphere WITHOUT aberration correction

Input OAM states

Output OAM states

Turbulent atmosphere

(b) Propagation through turbulent atmosphere WITH aberration correction

Input OAM states

Output OAM states
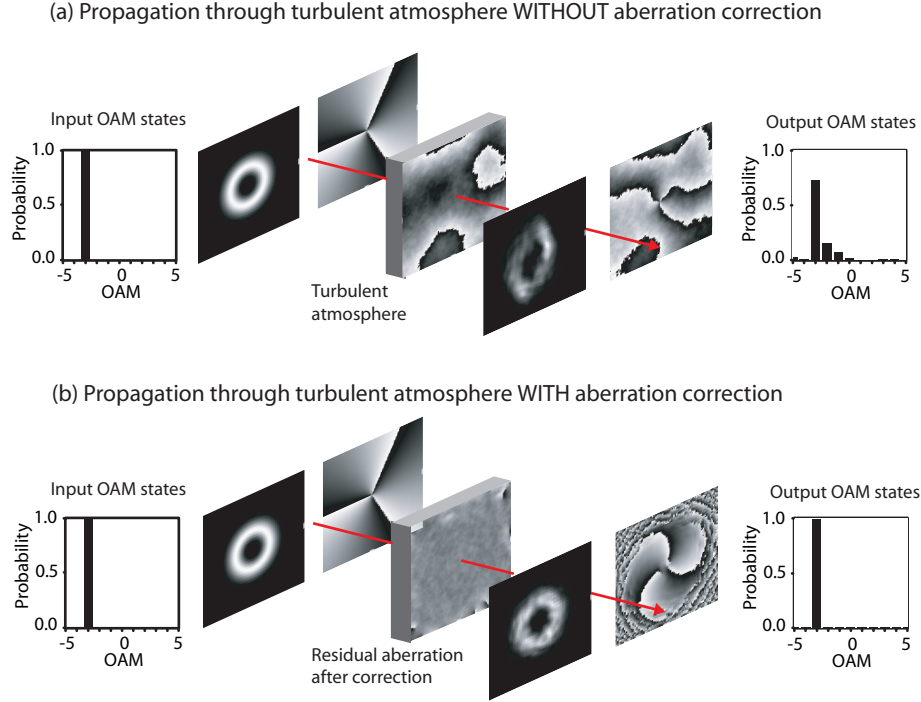
Residual aberration after correction

Fig. 1. The aberration caused by atmosphere turbulence and the mitigation effect of the aberration correction methods. (a) propagation through turbulent atmosphere without aberration correction (b) propagation through turbulent atmosphere with aberration correction.

3. Simulation results

In this section, we will verify the mitigation effect of both correction methods by numerical simulations. We dicuss the cases with a single OAM state propagating through turbulence and a communication link caused by the atmosphere turbulence.

3.1. A single OAM state propagating through turbulence and its purity

Fig. 1 shows the aberration caused by the atmosphere turbulence and a single OAM state propagating through turbulent atmosphere with and without aberration correction. The parameters for the simulation of atmosphere turbulence are the following: $C_n^2 = 5 \times 10^{-13} \mathrm{m}^{-2/3}$, $L_0 = 50\mathrm{m}$, $l_0 = 0.0002\mathrm{m}$, $N = 140$, $\Delta x = 0.0003\mathrm{m}$, and $\Delta Z = 50\mathrm{m}$. In the simulation, there are supposed five phase screens during the beam propagation. The results show that the purity of the input OAM state, $l = -3\hbar$, is damaged by the turbulent atmosphere, and the OAM state can be recovered by an aberration correction method.

In order to express the damaged effect of atmosphere turbulence and the recovery impact of aberration correction, we use decomposition in Fig. 1. Since LG modes are an orthogonal set of functions, they will compose a complete basis. Any state can be decomposed using this orthogonal basis, which is

$$\Psi(r,\theta,z) = \sum_p \sum_l a_{p,l}(z) LG_{p,l}(r,\theta). \tag{11}$$

The probability of obtaining a measurement, $l_z = \ell\hbar$, is obtained by summing all probabilities

associated with that eigenvalue

$$P(l) = \sum_{p} \left| a_{p,l}(z) \right|^2,$$ (12)

where the superposition coefficients $a_{p,l}(z)$ are given by the inner products

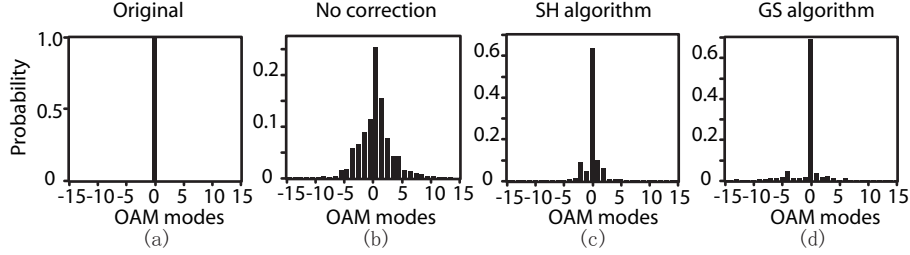$$a_{p,l}(z) = \left\langle LG_{p,l}(r,\theta) | \Psi(r,\theta,z) \right\rangle.$$ (13)

Fig. 2. Decomposition of the beam after passing through atmospheric turbulence with and without a correction. (a) original decomposition (b) without a correction (c) corrected by the Shark-Hartmann wavefront correction method (d) corrected by the phase correction method for OAM states.

In order to compare the mitigation effect of SH-algorithm and GS-algorithm presented in section 2, Fig. 2 shows the decomposition of the received state with the two correction methods in strong aberration case. The results show that for OAM $\ell=0$ state, the probability of the OAM state keeping on $\ell=0$ is only 25.3% in the atmospheric turbulence enviroment with $C_n^2 = 1 \times 10^{-12} \mathrm{m}^{-2/3}$, $L_0 = 50\mathrm{m}$, $l_0 = 0.0002\mathrm{m}$, $N = 128$, $\Delta x = 0.0003\mathrm{m}$, $\Delta Z = 100\mathrm{m}$. This probability can be improved to 63.8% by using SH-algorithm, where 12th order of Zernike polynomials have been used to estimate the wavefront. And this probability can be enhanced to 69% by using GS-algorithm. The results show that the two aberration correction methods have improved the beam quality significantly, then the phase correction method for OAM states show a better performance.

3.2. A communication system on OAM and its capacity

As discussed above, it is known that a single LG mode state will be polluted by turbulent aberration when it passes through atmospheric turbulence in free space. For a communication link based on OAM, turbulent aberrations may cause noise to the original OAM state. It is important to estimate the probability of keeping the original state in this communication channel [8–10].

Fig. 3 shows that the probability of keeping original OAM state varies with the strength of turbulent aberration. The results show that the probability of obtaining the original LG mode (corresponding to $\Delta = 0$) decreases as C_n^2 increases. At the same time, the probability for shifting to adjacent one LG mode ($\Delta = \pm 1$) is higher than those to shift to two ($\Delta = \pm 2$) or more modes. As the adjacent azimuthal modes increase, the probabilities of obtaining the original LG modes ($\Delta \neq 0$) decrease significantly.

Generally, channel capacity is regarded as a quality of a communication system. The noise caused by atmosphere turbulence can be described by a channel matrix $H = [H_{mn}]$, where the conditional probabilities H_{mn} can be evaluated by Eqs. (12) and (13). Here, m is the number of transmitted OAM states and n is the number of received states. For the simplicity, we select $\ell_m = 0, 1$ as the transmitted OAM states for $L = 1$ and the received OAM states are selected
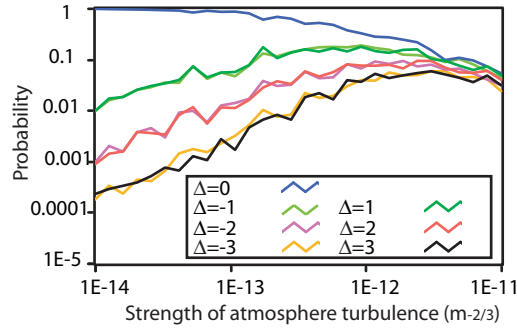
Fig. 3. The effect of turbulence on the propagating OAM quantum states as functions of C_n^2, where C_n^2 varies from $1 \times 10^{-14} \mathrm{m}^{-2/3}$ to $1 \times 10^{-11} \mathrm{m}^{-2/3}$, representing the strength of turbulent aberration changing from weak to strong. The distance of propagating is 100m, the outer scale is 50m, and the inner scale is 0.0002m. The simulation grid comprises 128×128 elements, and the grid spacing size is 0.0003m.
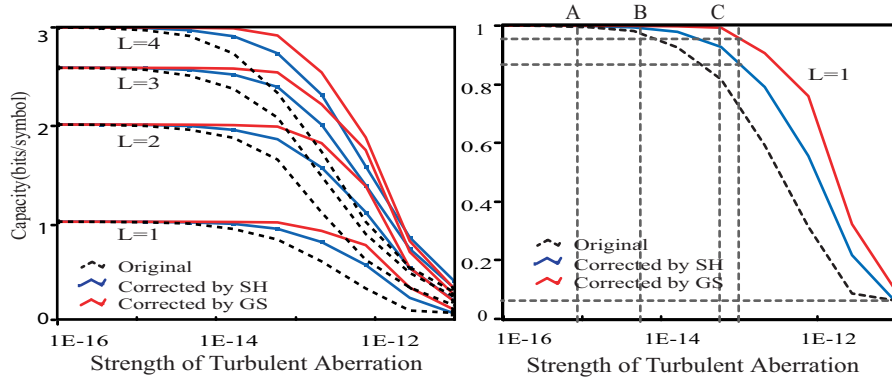

Fig. 4. Comparison of the channel capacity for a communication link employing OAM states of single photon through atmospheric turbulence, corrected by Shark-Hartmann wavefront correction method and the phase correction method for OAM states.

from $\ell_n = -15$ to $\ell_n = 15$. Similarly, we will select $\ell_m = 0, 1, 2, 3$ for $L = 2$ and decompose the received state from $\ell_n = -15$ to $\ell_n = 15$. We use the same scheme for $L = 3$ and $L = 4$. After we obtain the channel matrix, we can calculate the capacity of this discrete channel by the Blahut-Arimoto algorithm [23]. Fig. 4 shows the channel capacities for communication systems using different LG modes propagating through atmospheric turbulence with and without the two correction methods. The results show that the channel capacities decrease rapidly as C_n^2 increase, and both the correction methods can improve the channel capacities effectively. For example, atmosphere turbulence causes the capacity of two input OAM states ($L = 1$) to decrease from 1 bits/symbol to 0.08 bits/symbol when the structure constant of the index refraction varies from $1 \times 10^{-16} \mathrm{m}^{-2/3}$ to $1 \times 10^{-11} \mathrm{m}^{-2/3}$. The decreasing point A means atmosphere turbulence will cause noise to the communication channel at $C_n^2 = 9 \times 10^{-16} \mathrm{m}^{-2/3}$. SH-algorithm has postponed this decreasing to point B, where $C_n^2 = 7.5 \times 10^{-15} \mathrm{m}^{-2/3}$, and GS-algorithm has changed to $C_n^2 = 7 \times 10^{-14} \mathrm{m}^{-2/3}$ (point C). In other words, the capacity of the communication

channel will be improved by both the correction methods. For $L = 1$ and $C_n^2 = 1 \times 10^{-13} \text{m}^{-2/3}$ (a slight strong turbulent atmosphere), the capacity of a communication link in Fig. 4 is 0.725 bit/symbol. At this case, SH-algorithm has improved the capacity to 20.1% (0.875 bits/symbol), while GS-algorithm has enhanced this value to 0.96 bits/symbol (33%). Both correction methods have improved the purity of a single OAM state, and the capacity of a communication system on the OAM state significantly. Moreover, the phase correction method for OAM states is more effective for mitigating the turbulent aberrations.

4. Experimental results

From the above section, we find that the phase correction method for OAM states is more useful to overcome turbulent aberration in numerical simulations. On the other hand, if we use the observed intensity pattern in CCD as the deformation wavefront caused by turbulent aberration to Gerchberg-Saxton algorithm [22], the phase correction method for OAM states can be implemented experimentally. Therefore, we will discuss the effect of the phase correction method for OAM states as has been shown by the following experiments.

4.1. Experimental setup

Because LG modes of small helical charge have high sensitivity to the phase errors, even small phase irregularities cause significant deviations from their rotational symmetric 'doughnut' shape, we utilize $\ell = 1$ LG mode to determine the 'hologram' of the turbulent atmosphere aberration from the distorted shape of a focused doughnut mode. Unfortunely, this mode does not explain the change numerically. In order to illustrate the improvement of the phase correction method for OAM states to the turbulent aberration, we will design a referenced spot mode ($\ell = 0$) besides the doughnut, and we will use the participation function (also named as sharpness metric) to measure the spot quality. The participation function of the referenced spot is defined as following

$$P = \frac{\left(\Sigma_{i,j}^N I_{i,j}\right)^2}{\Sigma_{i,j}^N I_{i,j}^2}, \tag{14}$$

where $I_{i,j}$ is the intensity of the $(i,j)^{th}$ pixel of the referenced spot. It is shown that the smaller value corresponds to the more tightly focused spot [24].
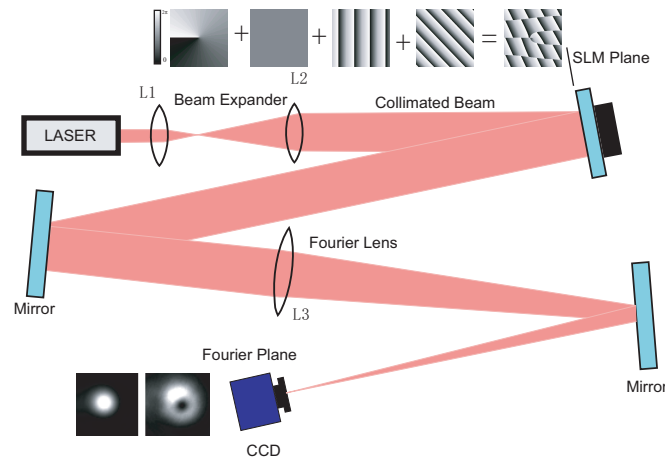

Fig. 5. The sketch of the experimental setup.

Fig. 5 shows the experimental system to test the turbulent aberration correction method. The reflective computer-controlled spatial light modulator shows a diffractive vortex lens, which transforms a collimated laser beam into an optical vortex of helical charge ℓ ($\ell = 1$ in the Fig. 5) and a referenced spot ($\ell = 0$) under somewhat turbulent aberration. As usual, the vortex lens is superposed by a grating in order to spatially separate the optical vortex generated in the first diffraction order from other orders. In order to detect the referenced spot besides the LG mode, different grating is assigned to LG mode and the referenced spot. The Fourier plane corresponds to the far-field diffraction pattern. A len (L_3) is used to focus the image on CCD in the Fourier plane, and several mirrors are arranged so as to get the biggest image in CCD as possible.

4.2. improvement of the participation function

At first, we get a deformed doughnut and referenced spot when we include phase screen from the simulations about the turbulent aberration on the SLM, then we use the phase correction method for OAM states to obtain the "correction hologram" of the turbulent aberration, and add it on the SLM. Finally, we can get an improved doughnut and referenced spot in CCD. The participation function of the reference spot with and without the correction method show the improvement of the correction method. In order to calculate the participation function with and without the correction method, we divide the CCD into two interesting areas, one for showing the correction procedures ($\ell = 1$ LG mode), and one for participation function calculations (($\ell = 0$ LG mode).

According to the atmosphere turbulence model, the random phase screen caused by atmosphere turbulence is mainly determined by the constant of the index of refraction. In order to understand the mitigation effect of the correction method, we measure the participation function of referenced spot with and without the correction method. We let the index of refraction change while keeping the other simulation parameters be constant during the experiments. Since the phase screen caused by atmospheric turbulence is random, phase screen obtained from the simulation is different from time to time, even with the same simulation parameters. We give the average value of the participation function in each case over 20 values.
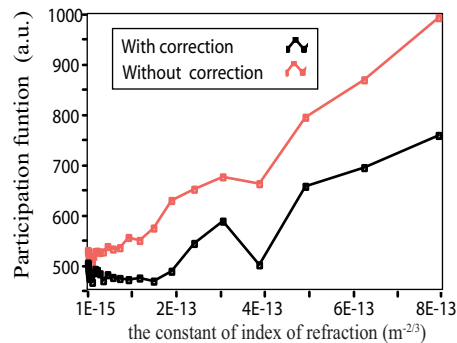

Fig. 6. The variance of the participation functions for the reference spot with the change of the index of refraction by the phase correction method for OAM states.

Fig. 6 shows the variances of participation function with the constant of index of refraction varying from 10^{-15} to 10^{-12}. The experimental results show that the values of participation function go down with the correction method, and the correction method is an effective way to mitigate the turbulent aberration. We get 45% maximum improvement and 17% average improvement by the change of strength of aberration.

5. Conclusion

In this work, we apply different aberration correction techniques [19, 21] to mitigate the deformation effect caused by the atmosphere turbulence. One is the Shack-Hartmann wavefront correction method, and the other is a phase correction method for OAM states. To quantify the improvements we calculate the channel capacities in a similar fashion to the method described in [8]. Our simulation results show that it is possible to recover the damaged LG mode caused by the atmosphere turbulence. The two correction methods have improved the purity of a single photon LG mode and the capacities of the free space optical communication channel produced by atmosphere turbulence significantly, and the phase correction method for OAM states outperforms the Shack-Hartmann wavefront correction method.

Using SLM, the phase correction method for OAM states is easier to implemented. We testify the correction method in a series of experiments. The experimental results show that the values of participation function decrease with the phase correction method for OAM states. The correction method is an effective way to mitigate the turbulent aberration both in simulations and experiments.